Bulletin of the Seismological Society of America, Vol. 99, No. 2B, pp. 1207–1214, May 2009, doi: 10.1785/0120080086

The Application of Fiber Optic Gyroscopes for the Measurement of Rotations in Structural Engineering

by K. U. Schreiber,* A. Velikoseltsev, A. J. Carr, and R. Franco-Anaya

Abstract The effects of rotations have been neglected in studies on the seismic properties of civil engineering structures in the past. This was mainly because their influence was thought to be small and there were no suitable sensors available to measure the system response of buildings to rotations properly. Only the effects of torsions caused by asymmetries in buildings, where the center of stiffness differs from the center of mass, are known from differential measurements of accelerometers. Different types of inertial rotation sensors exploiting the Sagnac effect have now reached the necessary sensitivity to be used for the investigation of rotational excitations in buildings. Because large ring lasers (Schreiber *et al.*, 2003, 2004) have successfully recorded signals of earthquake induced rotations from teleseismic events (Igel *et al.*, 2005), it is now time to study the behavior of buildings with respect to rotations. Fiber optic gyroscopes (FOGs) are commonly used for applications in inertial navigation. They are exploiting the Sagnac effect in a passive optical interferometer design in order to measure rotations with high precision. For that reason, these gyros can measure absolute rotations and do not require a specific frame of reference. Because the concept of operation is entirely based on optical signals, there are no mechanical moving parts inside the sensor, so the transfer function is constant and the system works over a very wide range of excitation frequencies (10^{-3} Hz $< f_{\mathrm{FOG}} <$ 2 kHz). Furthermore, one can obtain a well-defined reference to north from an FOG, which provides the additional advantage of using these sensors for the long term monitoring of structural stability. In this article we report initial measurements with an FOG on a shake table as well as results from *in situ* applications in very tall structures.

Introduction

Highly sensitive rotation sensors have many uses. They reach from applications in robotics over navigation up to high-resolution measurements in seismology, geodesy, and geophysics. The field of these applications is very broad and, therefore, a wide range of different sensor types and specifications exist to satisfy these demands. In order to understand the importance of rotation sensors, one should keep in mind that there are in total 6 degrees of freedom of movement, three for translations and three for rotations. While the measurements of translation are usually based on the determination of accelerations relative to an inertial test mass, rotations can be established either from mechanical gyroscopes or the absolute value can be measured by exploiting the Sagnac effect.

Today fiber optic gyros are the most prominent representatives for passive optical Sagnac interferometers; while ring laser gyroscopes represent the group of active Sagnac devices. They characterize the most sensitive and most stable class of gyroscopic devices. However, ring laser gyroscopes are large and very delicate to operate; in comparison, a fiber optic gyroscope (FOG) is small and robust, and the available sensor sensitivity is fully sufficient for the investigation of the behavior of tall buildings under the influence of wind load and earthquakes. The operation principle of an FOG is fairly simple; while the actual sensor design is highly complex in order to obtain high-sensor stability and resolution (Lefevre, 1993). Figure 1 illustrates the basic concept. A narrow spectral line width light beam[1] is generated by a light source (S) and passed on to an equal intensity beam splitter. The resultant two light beams are guided around a monomode fiber coil in the opposite direction. After passing through the fiber, both beams are superimposed again by the same beam splitter and steered onto a photodetector (D). If

*Present address: Department of Physics and Astronomy, University of Canterbury, Christchurch 8020, New Zealand

[1]Ideally a monochromatic laser beam would be required, but due to substantial interference as a result of scattered light this is not possible.

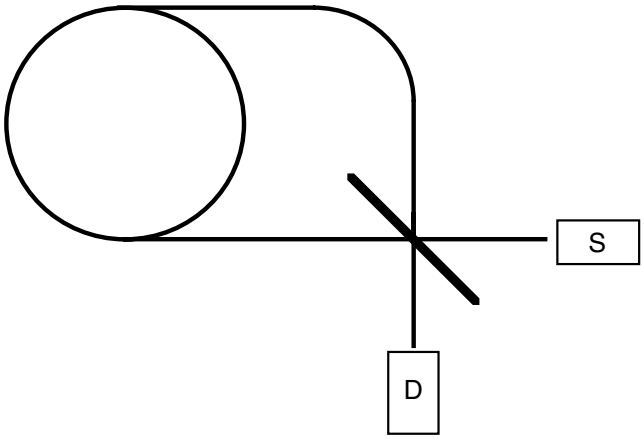

Figure 1. Operation principle of an FOG.

the entire apparatus is at complete rest, each of the beams travels the same distance, and there is no phase difference between the two beams. However, if the FOG is rotating about the normal vector on the fiber coil, the two beams do not travel the same distance and a small phase shift between the light beams is observed. Because the signals travel at the speed of light, the obtained phase shift remains very small. Therefore, a modulation technique, pulsed operation, and $\pi/2$ phase shifting for one sense of propagation are employed to achieve a maximum in instrumental sensitivity. Furthermore, the sensor is operated in a closed loop configuration in order to ensure a wide dynamic range. Details on the general sensor design of fiber optic gyros are given in Lefevre (1993) and are beyond the scope of this article.

A full description of the Sagnac effect is based on general gelativity (Höling, 1990), but in this case a classical interpretation yields the same result (Milonni and Eberly, 1988). The observed phase difference is

$$\delta\phi = \frac{8\pi A}{\lambda c}\mathbf{n}\cdot\boldsymbol{\Omega}, \tag{1}$$

where A is the area circumscribed by the light beams, λ the optical wavelength, c is the speed of light, $\mathbf{n}$ is the normal vector upon A, and $\boldsymbol{\Omega}$ is the rate of rotation of the interferometer. Equation (1) relates the obtained phase difference to the rate of rotation of the entire apparatus and can be interpreted as the gyroscope equation (Stedman, 1997). FOGs are modern representatives of this kind of optical gyroscopes. Because glass fibers with a length of several hundred meters are used, the scale factor can be made very large by winding the fiber to a coil, and the sensitivity for rotational excitations is, therefore, much larger than for a single loop. In this way even the Earth's rotation can be continuously observed to an accuracy of about 10%, even on a relatively modest FOG of about the size of a small cell phone.

Equation (1) can be rewritten as equation (2), substituting the area A for the length of the fiber L and the radius of the coil R:

$$\delta\phi = \frac{4\pi LR}{\lambda c}\mathbf{n}\cdot\boldsymbol{\Omega}. \tag{2}$$

While the scale factor $4\pi LR/\lambda c$ determines the sensor specific sensitivity of the gyro, the inner product $\mathbf{n}\cdot\boldsymbol{\Omega}$ gives the orientation of the sensor relative to the vector of rotation. Both quantities, the rate of rotation as well as the sensor orientation, are useful for the application of an FOG in structural engineering. In practical application, we read the instantaneous rate of rotation in the units of degrees per second at a preset rate of 100–4000 Hz from the serial port of the FOG.

Rotations in Structural Engineering

In the design of structures to resist seismic excitation, the current design approaches use only the input associated with ground accelerations. These usually only consider the two orthogonal horizontal (translational) ground acceleration components. The argument is that the structure is already designed to carry the maximum vertical loading with a reasonable factor of safety. Under earthquake excitation the structure is assumed to be beyond the elastic limit (the factor of safety is therefore 1.0), and the structure is only carrying the likely, or long term, vertical load, which is generally taken as 30% to 40% of the maximum design vertical load. The vertical accelerations, from past earthquakes, are smaller than the horizontal components, on the order of two-thirds of the horizontal accelerations. In the past, information on ground rotations has not been available because suitable measurement instrumentation was lacking. Ground accelerations are relatively easy to measure and the instruments are inexpensive, easy to calibrate, compact, and robust.

Many design codes make allowances for torsional effects in structures as history has shown that torsional responses are likely to lead to catastrophic collapse, and the torsion loads are usually assumed to be a function of the horizontal or translational accelerations multiplied by some eccentricity of mass or stiffness in the structure. This is basically to allow for unknown distributions of mass as well as stiffness and strength in the structure. Some design codes have increased this value in an attempt to allow for some torsional excitation from the ground motion, even if these have not then been measured. If torsional (rotation about a vertical axis) motions become available, together with information on surface rocking motions, then the earthquake engineering community will have to work out how these are to be implemented in the design process. An FOG has the potential of providing the required rotational signal, while it is entirely insensitve to translations at the same time due to the fact that it uses the concept of Sagnac interferometry.

Rotations are important measures in structural responses. Any torsional response in a building will infer translational movement in components located away from the center of rotation and this will have to be added to the translations in those members associated with the horizontal

ground motions. The average rotation about a horizontal axis of column members in a structure is usually measured as the interstory drift. This is the difference in the horizontal displacement from one floor to the next and is usually divided by the interstory height to give an angle, usually expressed as a percentage of the story height. Many building codes (Berg, 1983) in less seismically active regions of the world use a 1% interstory drift as an upper bound on allowable drift in a design level earthquake. Other codes may allow drifts of up to 2.5% for a well-detailed ductile design (New Zealand Loadings Standard, 1983; 1992). The magnitude of the interstory drift is a measure of the damage expected in the structure due to the earthquake excitation (Algan, 1982; Sozen, 1983; Moehle, 1994). The measurements of torsional responses and interstory drifts are reasonably easy on small scale models on a shake table or in a laboratory but are much more difficult in real or prototype structures. The torsional response can be measured using a pair of accelerometers and then dividing the differences in the horizontal accelerations by the distance between them in a direction perpendicular to the measured motion. This then has to be integrated twice with respect to time to give the torsional rotations. However, this technique has some important limitations because of the inherent sensor drift and a small offset from zero in the absence of an input signal.

In a laboratory, displacement transducers could be used in a similar manner as is shown in the Shake-Table Measurements section of this article. In a real structure only the accelerometers are available as there is no fixed frame of reference from which to take the measurements. The FOG device measuring rotational velocity is simple to use. Setup requires clamping the FOG to the floor, or some other suitable part of the structure, and connecting it to a computer and a power supply. Then one is ready to start measurements and integrate the rotational velocities to determine the rotations. There is no locating two instruments, carefully aligning their orientation, and checking the time and phase of the two instruments. Furthermore, an FOG also provides the correct angle of rotation when the center of rotation is a long distance from the sensor. In the case of the differential measurements of two or more accelerometers, the geometry of the measurement arrangement with respect to center of rotation is of great importance for the resolution of the measurement technique.

Similarly for measuring interstory drifts, it is, in principle, possible to arrange a frame from the floor below to near the ceiling above to set up displacement transducers to measure the difference in displacements. There have been suggestions of setting up a light source near the ceiling that is directed to a gridlike receiving device on the floor to detect movement of the light source (McGinnis, 2004); however, apart from the hardware complexity of this approach, it is also vulnerable to building deformations. Distortions may cause the light source to tilt, which would be amplified by the length of the light beam. This creates readout signals that in reality are not there. In a prototype building displacements have to be measured from floor to floor as no external reference frame is available. In a structures laboratory, or with a shake-table test of a structure, it is possible to mount displacement transducers at every floor to measure the displacements of the floors relative to a fixed reference frame. Again the FOG device provides a simple and reliable solution, one clamps, or affixes, the device to a column, usually at midheight, and the interstory drift velocities are recorded directly. These only require integrating with respect to time to give the interstory drifts.

Sensor Verification

At first the FOG test sensor μFORS-1 (serial number 1376, manufactured by Northrop-Gruman-LITEF GmbH[2]) was operated under static conditions. A series of scaled rotation rates in units of degrees per second, sampled at a rate of 1 kHz, were measured. Figure 2 shows one example of the obtained data sets. One can see how the inbuilt feedback filter loops optimize the measurement resolution after an initial reset. It takes about 5 sec to obtain a minimum noise level of $\pm 0.05°/\text{sec}$. By integration one obtains the specified sensor sensitivity of $0.001°/\text{hr}$ as specified by the manufacturer. In order to check the spectral response from the gyroscope, several power spectra have been taken from the static recordings. A typical spectrum of the FOG, rigidly placed on the ground, is shown in Figure 3. As expected the spectrum has no distinct features over the entire Nyquist regime of $0 \leq f \leq 500$ Hz. The spectrum in Figure 3 shown in a logarithmic y scale, represents the important section out of a full spectrum taken over the entire regime up to the Nyquist limit. In order to check the sensor stability over a period of several hours, an Allan-deviation study has been carried out (Allan, 1987). This method employs a statistical approach to identify various sources of drift as a function of integration time. The data set was normalized to the mean value of all measurements for that purpose. The Allan-deviation plot is shown in Figure 4.

There are no systematic sensor drift effects for a time interval of integration with a duration of up to one day visible in Figure 4. The obtained slope of $s = -0.5$ is a clear indication for white noise as the only noise source present over the examined interval of time, which shows that the sensor drift is too small to be of any significance in the context of the applications outlined in this article. The increase of the scatter toward the right side of the plot is coming from the progressively smaller number of samples available for the averaging process as part of the Allan-deviation estimation and is rather a limitation of the method than a sensor effect. Therefore, one can conclude that it is possible to apply the μFORS-1 not only for dynamic studies, but also for longer term monitoring purposes.

[2]The retail price of this unit is about 6000 Euro, but cheaper versions with lower resolution also exist.

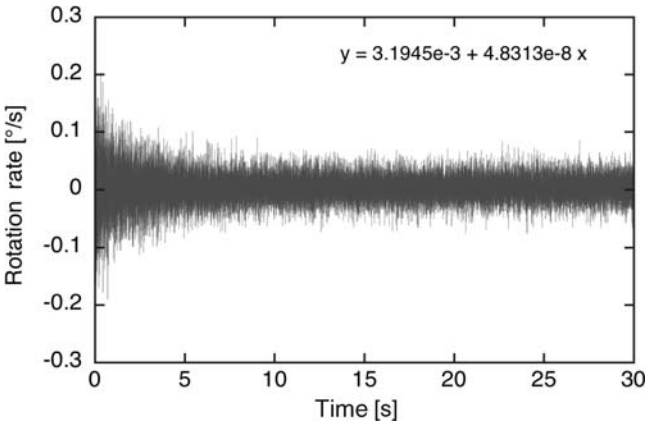

Figure 2. Time series of the rotation rate measured by an FOG μFORS-1 placed statically on the laboratory floor. The obtained offset of 3.1945×10^{-3} deg/sec corresponds to the Earth rotation rate observed from a horizontally orientated FOG at a latitude of about 49° (see equation 2).

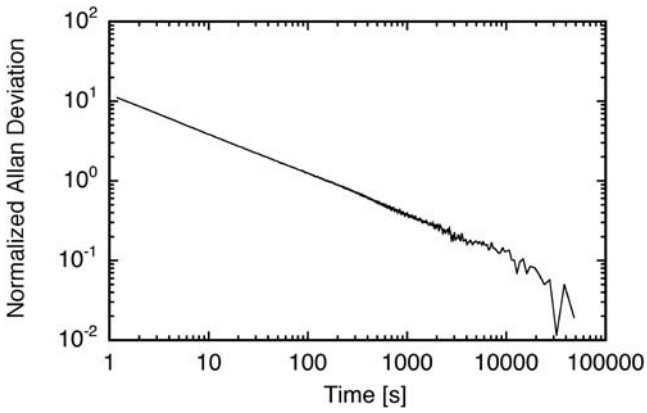

Figure 4. Allan-deviation of the μFORS-1 computed from a set of measurements taken on 24 October 2005. The data uncertainty is increasing noticeably toward the right-hand side of the diagram. This is due to the progressively smaller number of values for the averaging process as the length of the data sets increases; this is an effect inherent to this analysis technique.

Shake-Table Measurements

Shake-table tests on downscaled models of buildings are widely used for the study of their behavior during an earthquake of a given signature. Under these controlled laboratory conditions these tests can also include the precise measurement of interstory drift. For this purpose one can mount a rigid frame to the fixed laboratory floor. With several displacement transducers attached to this reference frame, it is possible to establish the movement of each location of the model being tested along the axis of translation of the shake table. Figure 5 shows one example of a four-story building model with a total of five transducers attached to the reference frame reaching over the shake table from the right-hand side of Figure 5. (The rectangular aluminum boxes are the transducers, while the gray painted metal profiles make up the support structure.) Because FOGs do not require an external frame, they can measure the interstory drift as a rotation around the normal vector on the fiber coil. For a comparison test we have attached the μFORS-1 vertically to the building model on the shake table at one of the columns halfway between the ground and first floor. Figure 6 shows the setup. In order to evaluate the suitability of the FOG for civil structures under seismic excitations, a series of shake-table tests were performed on the four-story model structure shown in Figure 5. The model structure was designed by Kao and is widely used for seismic testing at the University of Canterbury (Kao, 1998). A main feature of this steel moment-resisting frame structure is the incorporation of replaceable fuses located in critical regions of the structure to show the effects of inelastic structural performance under seismic loading. The model building is a 2.1 m high three-dimensional four-story frame structure. The frames are built using square hollow steel sections for beam and column

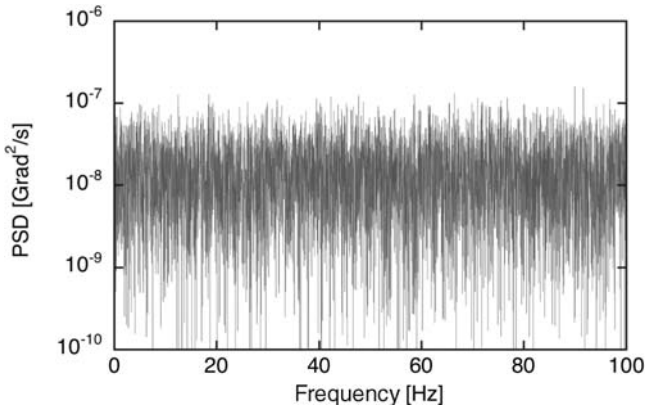

Figure 3. Spectrum from a measurement of a statically placed sensor. There are no systematic features visible over the entire Nyquist regime.

Figure 5. View of the shake table with a four-story model mounted on top. Reaching in from the right-hand side one can see five displacement transducers mounted on a reference frame fixed to the laboratory floor.

Figure 6. View of the installation of the FOG on the building model on the shake table.

members. The fuses, beam–column joints, and other connecting components are made of steel flat bars. Two frames in the longitudinal direction provide the lateral load resistance. Each frame has two bays with 0.7 and 1.4 m long spans. The short bay is to show earthquake dominated response, while the long bay is to show gravity dominated response by having an extra point load induced by a transverse beam at the midspan at each level.

In the transverse direction, three one-bay frames with a 1.2 m long span provide lateral stability and carry most of the gravity load. A oneway floor slab provides a significant proportion of the model mass. The slab is made of steel planks and is connected to a rigid steel plate that acts as a diaphragm. The planks are simply supported on the beams of the transverse frames and on the intermediate beam supported by the long span beams of the longitudinal frames (Fig. 5). The four-story model building was designed as a one-fifth scale structure. It was intended to model the structure as a typical four-story reinforced concrete frame building; therefore, the natural period of the model was required to be within 0.4 to 0.6 sec to obtain similar response under earthquake excitation (Kao, 1998).

The equivalent static method, outlined in the New Zealand Loadings Standard (NZS) (1993), was employed to calculate the earthquake forces. The seismic weight of the one-fifth scale structure is 35.3 kN. A structural ductility factor of 6 was adopted for the structural design. Thus, the model structure was designed for a base shear force of 8.7% of its seismic weight.

A number of earthquake signatures have been applied to the shake table and in all cases an excellent agreement between the two independent methods was found (Franco-Anaya *et al.*, 2008). Figure 7 shows the example of the Kobe earthquake, which was scaled down in magnitude to 10% of its original strength. As one can see from Figure 7 there is a very slight discrepancy between the displacement obtained from the transducers and the displacement computed from the measured rotation rate of the FOG at the peak values. It is believed that this is a systematic effect caused by deformations on the transducer arms under maximum strain. The data gaps are a result of a software problem in the data logger of the FOG, which was identified only later during the data analysis.

An assessment of the accuracy of the FOG's measurements is made by comparing the measurements obtained with the FOG and those provided by a conventional linear potentiometer from the fixed reference frame (Fig. 5). The column's rotation is obtained by numerical integration of the rotation rate measured by the FOG (without the need for an external reference frame). The floor displacement is then calculated by multiplication of the column's rotation by the height of the first floor. In the same way, the column's rotation is calculated with the inverse tangent of the displacement at the first floor, obtained by conventional potentiometers, divided by the story height. The rotation rate is then determined by numerical differentiation of the column's rotation.

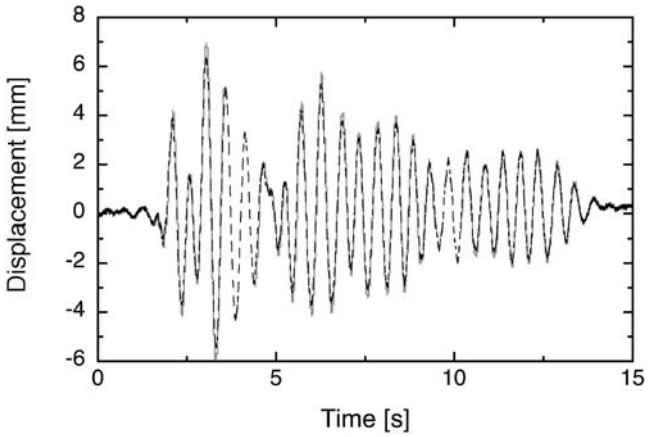

Figure 7. Comparison of the interstory drift of the first floor of a four-story model building on the shake table. The solid gray curve shows the displacements measured with a transducer from a laboratory fixed frame of reference, while the dashed curve shows the measurements from an FOG with no extra external reference. The gaps in the FOG data are unintentional and caused by a data logger problem.

Using the first floor for this comparison was done in order to demonstrate the measurement principle without the complication of building deflection and deformation. In a real world application one would have to apply more than one rotation sensor throughout the building. Observed differences between several sensors would in turn provide the benefit of identifying deflection and deformation, which would correspond to locations of energy dissipation.

Displacements of Static Structures

While this type of displacement transducer application is readily available in the laboratory environment, it is entirely impossible in a real world earthquake measurement scenario. However, for the applications of an FOG there is no difference between a laboratory experiment and, for example, the measurement of the rocking mode of a tall structure. Therefore, we have carried out measurements in one of the upper floors in the Sky Tower (328 m) in Auckland (New Zealand). Here, the device was clamped to antenna frames on the outside of the tower at level 54 and to window supports at level 60. It only took a few minutes to set up the instrument and to start taking readings from the Sky Tower. During a three day period of time, several measurement series with durations between 6 and 12 min were taken under calm wind conditions. Wind speeds varied between 24 and 36 km/h. The computer recorded the instantaneous rotation rate (degrees per second), as measured by the FOG at 1 msec intervals. The sensor was oriented such that it was sensitive to the rocking mode of the structure in the north–south direction. Figure 8 shows one sample out of approximately 20 data sets obtained over the 3 day period. The measured rotation rate was integrated to yield the excursion angles of the structure and then converted to a structural displacement as a high-resolution function of time. It can be seen that the typical excursions reach a level of about 2 cm peak to peak over periods of about 7 sec. The envelope of these excursion measurements shows the response of the Sky Tower to wind gusts. It is important to note that the measurements have a very good signal-to-noise ratio, despite the small overall values. A power spectrum was obtained from the displacement time history shown in Figure 9. The integral of the power spectral density over a given frequency band computes the average power in the signal over that frequency band. A resonance frequency of 0.165 Hz that corresponds to the rocking motion of the Sky Tower can clearly be seen in Figure 9 with good signal-to-noise ratio.

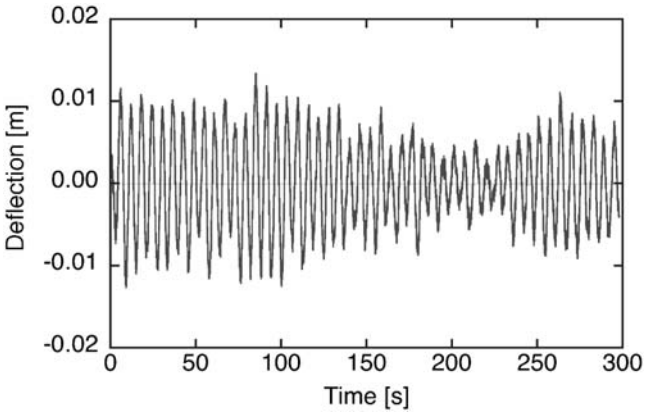

Figure 8. Measured displacement of the fifty-fourth floor of the Sky Tower. An oscillation with a period of 7 sec is clearly visible in the data with a good signal-to-noise ratio. The envelope shows the variation of the wind speed.

Displacement of Dynamic Structures

In the next step, the FOG has been applied to the investigation of the behavior of dynamic structures. For that purpose we have operated the μFORS-1 on a 70 m tall wind generator near Cuxhaven (Germany). Figure 10 shows the structure, which is usually operated at a rate of 20 revolutions of the wind turbine blades per minute. The FOG was operated under moderate conditions (wind speed 25–40 km/h) in three different orientations. In the first measurement series, the sensitive axis of the FOG was orientated parallel to the main shaft of the wind generator. Then it was rotated by 90°, so that the sensor was still orientated vertically, but in a direction parallel to the plane in which the blades were rotating. In the last measurement series the normal vector on the fiber coil of the FOG was pointed upward, so that the torsion around the horizontal plane could be measured. When the first measurement was carried out, the rotor blades were stopped so that the rocking mode of the structure under static conditions could be captured. As in the case of the Sky Tower measurements, we have taken the measured rotation rates and integrated them numerically once in order to obtain the angle of displacement as a function of time, which was then multiplied by the height of the sensor above ground. Figure 11 shows the result. The first mode of the structure has a frequency of 0.44 Hz and the observed amplitudes are on the order of up to 2 cm peak to peak. The power spectrum

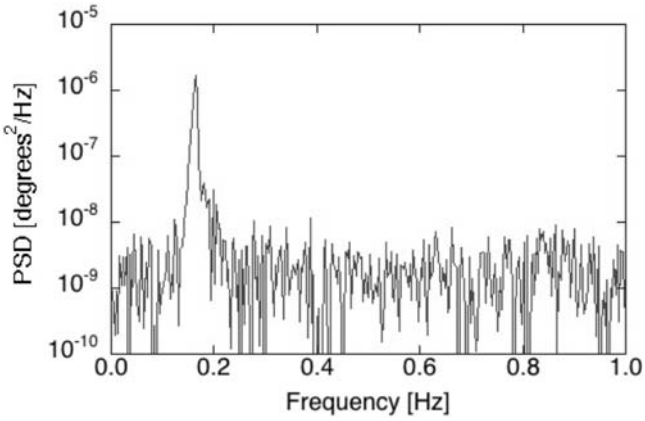

Figure 9. Power spectrum of the example of the displacement measurements of the Sky Tower. The rocking mode is excited with a frequency of 0.165 Hz.

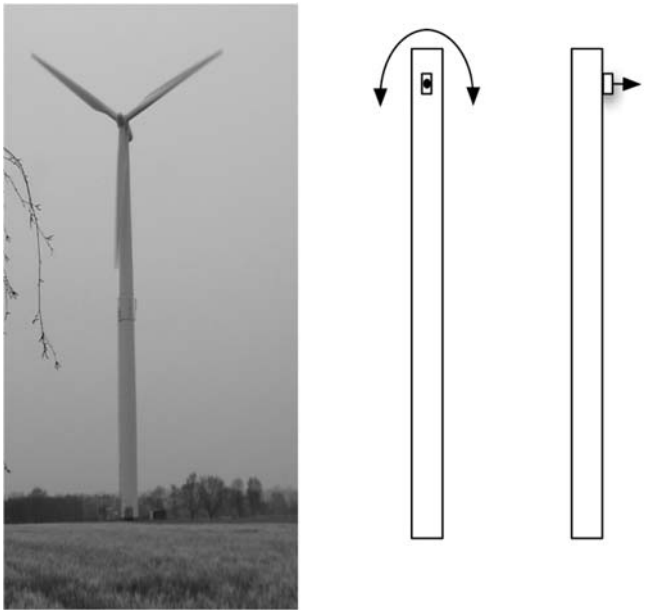

Figure 10. View of the wind generator in northern Germany near the city of Cuxhaven. The FOG is rigidly mounted to the tower structure near the rotor. The drawing in the middle of the figure shows the front view, and the drawing on the right-hand side of the figure indicates the side view. The actual installation is similar to that shown in Figure 6

in Figure 12 also shows that the second mode is excited at 3.04 Hz. Apart from that, there are no further frequency components evident in the data set.

When the wind generator was turned on, one could observe that the rocking of the tower showed larger excursions as well as that the higher frequency of 3.04 Hz now becomes noticeable. Furthermore, there is a clearly visible beat note between the first mode at 0.44 Hz and another low frequency at 0.36 Hz. This latter frequency is presumably caused by the first mode of oscillation of the rotor blades. Figures 13 and 14 show the respective diagrams. The first mode of the structure has a frequency of 0.44 Hz, and the observed amplitudes

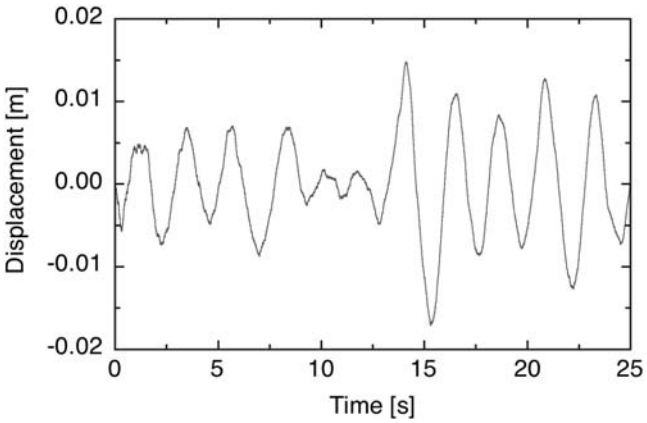

Figure 11. Measured displacement of the top of the wind generator about the main axis of the rotor.

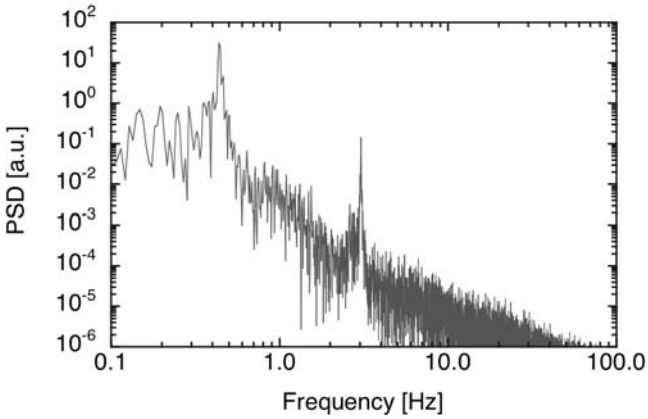

Figure 12. Power spectrum of the measured excursions as shown in Figure 11.

are on the order of up to 2 cm peak to peak. Another signal that also has started to show up is located around a frequency of 1 Hz and not as sharply defined as all previously mentioned signals. This signal can be associated with the effect of the rotor blades passing in front of the tower of the wind generator (three blades at a rate of 20 revolutions per minute).

Conclusion

FOGs have demonstrated their suitability for their application in structural engineering, in particular where no external reference is available to measure interstory drift, for example. FOGs are small, easy to use, and have sufficient sensitivity. Because they are entirely optical devices, they do not have the problems that characterize inertial mass transducers. Furthermore, they operate over a very wide range of mechanical oscillation frequencies. Applications reach from the static monitoring of building stability up to highly dynamic vibration measurements with frequencies of several hundred hertz. Their greatest strength is the fact that they measure absolute rotations or oscillations, so that they do

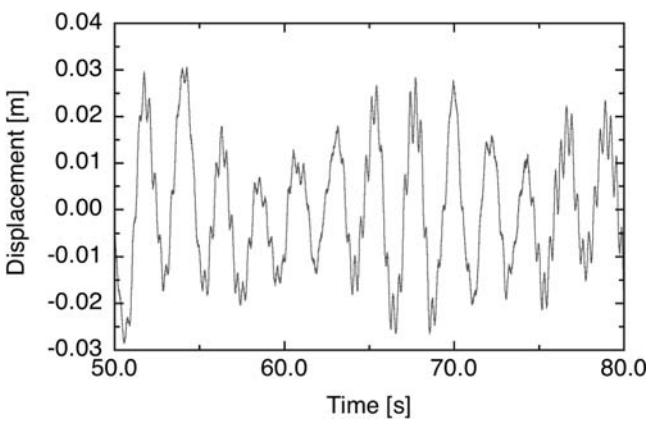

Figure 13. Measured displacement of the top of the wind generator about the main axis of the rotor.

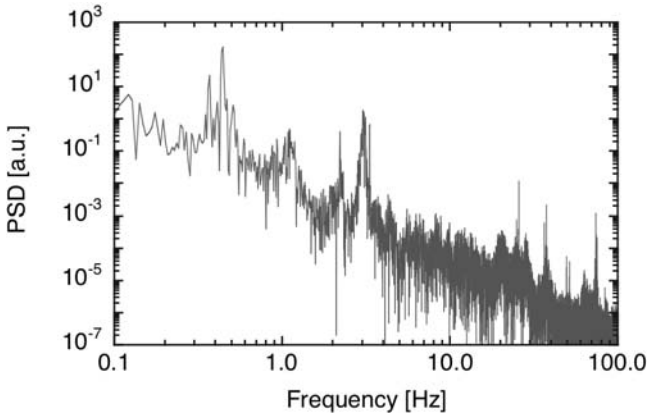

Figure 14. Power spectrum of the measured excursions as shown in Figure 13.

not require an external reference frame for their measurement. This means that FOGs measure true rotations even during an earthquake, where nothing remains static.

Data and Resources

All data used in this article were taken by the authors in various measurement environments.

Acknowledgments

This work was possible because of the collaboration between the Forschungseinrichtung Satellitengeodäsie, Technische Universität München, Germany, and the University of Canterbury, Christchurch, New Zealand. The authors would like to thank U. Hugentobler and G. Müller for their encouragement and support. Our special thanks go to Jan Ohlmann of Plambeck Neue Energien Betriebs-und Beteiligungs GmbH for making the wind generator measurements possible.

References

Algan, B. B. (1982). Drift and damage considerations in earthquake resistant design of reinforced concrete buildings, *Ph.D. Thesis*, University of Illinois, Urbana-Champaign.

Allan, D. W. (1987). Time and frequency characterization, estimation and prediction of precise clocks and oscillators, *IEEE J. Quantum Electron.* **6,** 647–650.

Berg, G. V. (1983). *Seismic Design Codes and Procedures*, Monograph of the Earthquake Engineering Research Institute, Berkeley, California.

Franco-Anaya, R., A. J. Carr, and K. U. Schreiber (2008). Qualification of fibre-optic gyroscopes for civil engineering applications, in *Proc. of the New Zealand Society of Earthquake Engineering (NZSEE) Conf. 2008*, Wairakei, New Zealand (available on CD-ROM).

Höling, B. (1990). Ein Lasergyroskop zur Messung der Erdrotation, *Ph.D. Thesis*, Universität Tübingen.

Igel, H., K. U. Schreiber, B. Schuberth, A. Flaws, A. Velikoseltsev, and A. Cochard (2005). Observation and modelling of rotational motions induced by distant large earthquakes: the *M* 8.1 Tokachi-oki earthquake September 25, 2003 *Geophys. Res. Lett.* **32,** L08309, doi 10.1029/2004GL022336.

Kao, G. C. (1998). Design and shaking table tests of a four-storey miniature structure built with replaceable plastic hinges, *Master's Thesis*, University of Canterbury.

Lefevre, H. (1993). *The Fiber-Optic Gyroscope* Artech House, Boston.

McGinnis, (2004). Apparatus and method for detecting deflection of a tower, U.S. Patent application number 0107671 A1, filed 10 June 2004.

Milonni, P., and J. Eberly (1988). *Lasers*, Wiley, New York, 589ff.

Moehle, J. P. (1994). Seismic drift and its role in design, *Proc. of the 5th U.S.–Japan Workshop on the Improvement of Building Structural Design and Construction Practices*, San Diego, 65–78.

New Zealand Loadings Standard (NZS) (1983). *Specification for Seismic Resistance of Engineering Systems in Buildings*, NZS 4219:1983, Wellington, New Zealand.

New Zealand Loadings Standard (1993). *Code of Practice for General Structural Design and Design Loadings for Buildings*, NZS 4203:1992, Wellington, New Zealand.

Schreiber, K. U., G. E. Stedman, and T. Klügel (2003). Earth tide and tilt detection by a ring laser gyroscope, *J. Geophys. Res.* **108,** no. B2, 2132, doi 10.1029/2001JB000569.

Schreiber, K. U., A. Velikoseltsev, M. Rothacher, T. Klügel, G. E. Stedman, and D. L. Wiltshire (2004). Direct measurement of diurnal polar motion by ring laser gyroscopes *J. Geophys. Res.* **109,** no. B6, B06405doi 10.1029/2003JB002803.

Sozen, M. A. (1983). Lateral drift of reinforced concrete structures subjected to strong ground motion, *Bull. New Zealand Natl. Soc. Earthq. Eng.* **16,** no. 2, 107–122.

Stedman, G. E. (1997). Ring-laser tests of fundamental physics and geophysics, *Rep. Prog. Phys.* **60,** 615–688.

Technische Universitaet Muenchen
Forschungseinrichtung Satellitengeodaesie
Fundamentalstation Wettzell
93444 Bad Kötzting, Germany
schreiber@fs.wettzell.de
(K.U.S., A.V.)

Department of Civil and Natural Resources Engineering
University of Canterbury
Private Bag 4800
Christchurch 8020, New Zealand
(A.J.C., R.F.)

Manuscript received 25 May 2008